Mechanical based alignment of large optical instruments: ESPRESSO as an example

G. Pariani, M. Aliverti, M. Genoni, L. Oggioni, M. Riva, et al.

G. Pariani, M. Aliverti, M. Genoni, L. Oggioni, M. Riva, S. Santana Tschudi, D. Mégevand, S. Cristiani, F. Pepe, "Mechanical based alignment of large optical instruments: ESPRESSO as an example," Proc. SPIE 10706, Advances in Optical and Mechanical Technologies for Telescopes and Instrumentation III, 107064H (10 July 2018); doi: 10.1117/12.2313180

SPIE.

Event: SPIE Astronomical Telescopes + Instrumentation, 2018, Austin, Texas, United States

Mechanical based alignment of large optical instruments: ESPRESSO as an example

G. Pariani[a*], M. Aliverti[a], M. Genoni[a], L. Oggioni[a], M. Riva[a], S. Santana Tschudi[b], D. Mégevand[c], S. Cristiani[d], F. Pepe[c]
[a]INAF, Osservatorio Astronomico di Brera, via E. Bianchi 46, 23807 Merate (Italy);
[b]European Southern Observatory, Paranal Observatory (Chile); [c]Observatoire Astronomique de l'Université de Genève Sauverny, Chemin des Maillettes, 51 CH-1290 Versoix (Switzerland);
[d]INAF, Osservatorio Astronomico di Trieste, Basovizza 302, 34149 Trieste (Italy).

ABSTRACT

When long term instrument stability is required, traditional alignment techniques based on bulky and/or flexible mountings can not be used due to their reduced stiffness. Mechanical alignment of optical systems is nowadays possible thanks to different 3D Coordinate Measuring Machines, as the Laser Tracker, the Articulated and Cartesian Arms. In this paper we describe the methods we considered for the integration and alignment of ESPRESSO, the very high resolution visible spectrograph for the ESO VLT, now under commissioning phase at Paranal Observatory. Different examples of the Front End (FE), the Anamorphic Pupil Slicer Unit (APSU), and the spectrograph itself will be provided, to demonstrate that it is possible to align an optical system with mechanical methods with minimal optical feedbacks, reaching in an almost 'blind' way the best optical performances.

Keywords: Mechanical alignment, high resolution spectroscopy, ESPRESSO, integration, verification

1. INTRODUCTION

Traditional alignment techniques usually rely on optical feedbacks to position the elements over all the required degrees of freedom. Bulky and/or flexible mountings with push-pull screws are usually considered to align the elements and then fix their position. This approach can not be followed when a long term stability of the instrument is required, due to the reduced stiffness and robustness of the mountings. The recent developments of different 3D Coordinate Measuring Machines, as the Laser Tracker (LT), the articulated and Cartesian arms, have brought their measuring accuracy at the micrometer level on the meter-size measuring scale, opening the way to the mechanical alignment of the elements in the AIV phase of optomechanical systems.
These instruments have been extensively used for the integration and alignment of ESPRESSO[1–3], the very high resolution spectrograph for the ESO Very Large Telescopes (VLTs), from the very beginning of the design phase to map the Paranal infrastructure up to the integration of the smallest subsystems. ESPRESSO is a fiber-fed, pupil-sliced, two-arms cross-dispersed echelle spectrograph placed in vacuum and in a multiple shells' thermal enclosure. It is a widespread instrument at the observatory, working either with a single Unit Telescope (UT) or with multiple UTs. In fact, the instrument is installed in the Combined Coudé Laboratory (CCL) and receives the light from the UTs through the four Coudé Trains (CT)[4] and the Front End (FE)[5], which injects the light into the optical fibers connected to the spectrograph. The instrument concept is shown in Figure 1.
Concerning the FE, it exploits a modular concept[5,6]. It is made by four identical units-module (FE Unit), receiving the beam from the relative telescope CT and the calibration light from the calibration unit. On the other side, the FE Unit feeds the fibers that carry the light to the spectrograph, corresponding in number and size to the scientific observing modes conceived for ESPRESSO[1–3]. Each FE Unit provides field and pupil stabilization via piezoelectric tip/tilt mirrors driven by a reimaging system. A toggling system, called mode selector, is provided to switch between the different observing modes and to inject the beam into the fibers (two for each observing mode) through the Fiber Link (FL). The light is then scrambled and provided to the spectrograph.

*giorgio.pariani@brera.inaf.it

Advances in Optical and Mechanical Technologies for Telescopes and Instrumentation III, edited by Ramón Navarro, Roland Geyl, Proc. of SPIE Vol. 10706, 107064H · © 2018 SPIE
CCC code: 0277-786X/18/$18 · doi: 10.1117/12.2313180

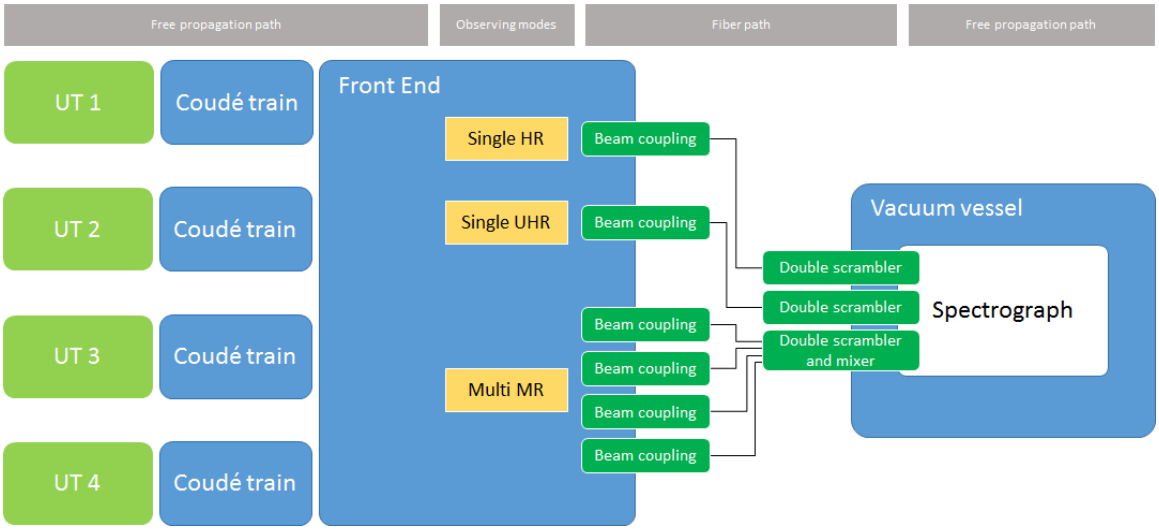

Figure 1: Conceptual scheme of ESPRESSO

Concerning the spectrograph, it is a two channel cross-dispersed echelle spectrograph[7]. The pupil is resized and sliced by the Anamorphic Pupil Slicer Unit (APSU)[8], which also converts the light into a f/15xf/10 beam. The light is than collimated to the size of the Echelle Grating (ECH) mosaic (three tiles of 400x200 mm, R4, 31.6 lines/mm) by an off-axis parabolic mirror of 700x380 mm, called Main Collimator (MC). The MC is used in double pass, to collect the dispersed light from the grating towards the transfer optics. A dichroic splits the light in the blue and red arms, than it is re-collimated by the corresponding Transfer Collimator (TC) to project a white pupil on the grism cross-disperser, based onto a volume-phase holographic (VPH) grating. After the grism, the 150x150 mm pupil is focalized onto the 9x9k, 10 um pixel width CCD with a refractive camera, F/2.7 and 10 degrees FoV, composed by a cemented doublet and two singlets, with two aspherical surfaces. The overview of the spectrograph and the optical design layout are reported in Figure 2.

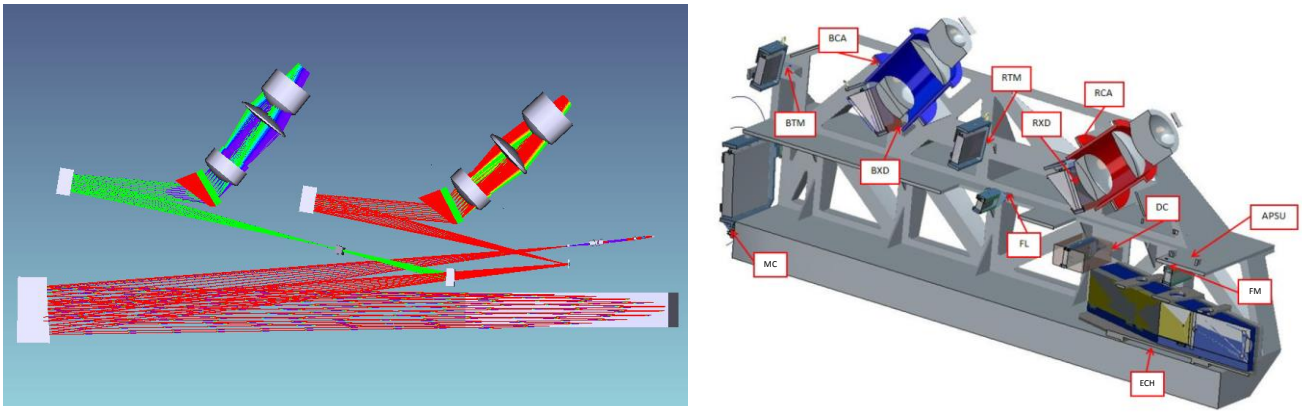

Figure 2: Left: spectrograph optical scheme. Right: Optical bench and optical elements - APSU: anamorphic pupil slicer unit, MC: main collimator, ECH: Echelle grating, DC: dichroic mirror, FM: field mirror, FL: field lens, BTM/RTM: blue/red transfer mirrors, BXD/RXD: blue/red cross dispersers, BCA/RCA: blue/red cameras.

Given the complexity and diversity of the spectrograph subsystems, the different instruments have been used in combination as function of the measuring range and required level of accuracy. In general, large components as the Paranal infrastructure, the FE structure, and the spectrograph optical bench have been measured with the laser tracker (LT, Vantage e_{ADM}=16µm+L*0.8µm/m). For the optical components, the mechanical metrology was performed through an anthropomorphic arm (FARO Arm EDGE) with a volumetric error of 41 um for the integration of the single elements, and a dedicated Coordinate Measuring Machine (CMM, COORD3 Universal) with a MPE_L of 1.8+L/333 um

for the metrology of the single mountings. The technique is based on the dimensional characterization of every optical element with respect to referencing points on their mounts. The same points are measured and aligned to the desired position during integration, adjusting with metallic shims the semi-kinematic mounting (see Figure 3). In case of complex components of the APSU, an hybrid optical-mechanical technique was used to properly define the mechanical references.
In the following sections, after a brief resume of the techniques considered, we will describe the optical verifications performed. The corrections applied during the optical verification are considered as the accuracy of the blind mechanical alignment. Examples where these methods could not be applied will be also shown to highlight their limitations.

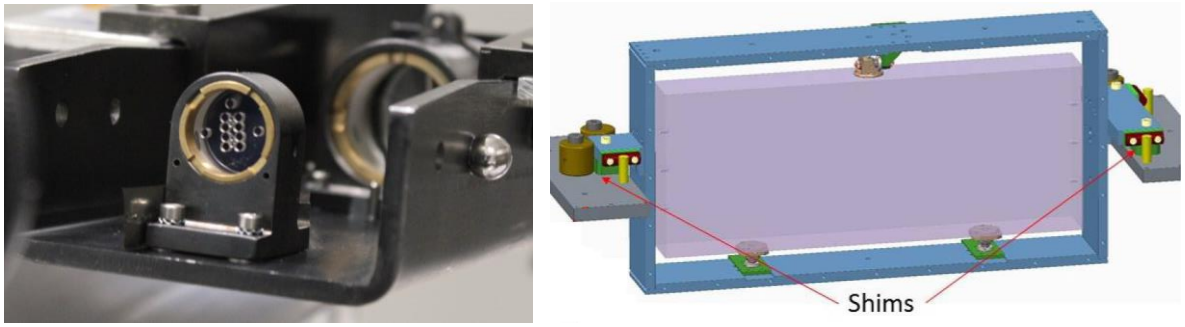

Figure 3: Left: reference sphere on the APSU bench. Right: spectrograph optics mounting[9].

2. FRONT END UNIT

The FE has been designed as a modular system, to be interchangeable between the different UTs. Accordingly, the alignment strategy consisted of three main steps:

- in laboratory, the alignment and integration of the different FE Units was performed with a combination of the anthropomorphic arm and CMM on a common optical and mechanical reference. The kinematic mounts of each FE bench were used as mechanical reference for the single unit, while a telescope simulator was constructed to act as optical reference. In this way, the kinematic mounts of all units were univocally positioned as respect to the desired optical axis. We estimated a maximum alignment error of the kinematic mounts from their nominal position of 100 um. Details are reported in a previous proceeding[10].
- at Paranal, the alignment of the main structure, mode selector and FE kinematic mounts as respect to the four telescopes convergence point were performed with the laser tracker[11]. Kinematic mounts were aligned with a maximum error of 112 um PV.
- at Paranal, the alignment of the Fiber Links as respect to the different FEs for the different observing modes (HR, UHR, and four MR heads) were performed with the feedback of the field and pupil cameras of each FE.

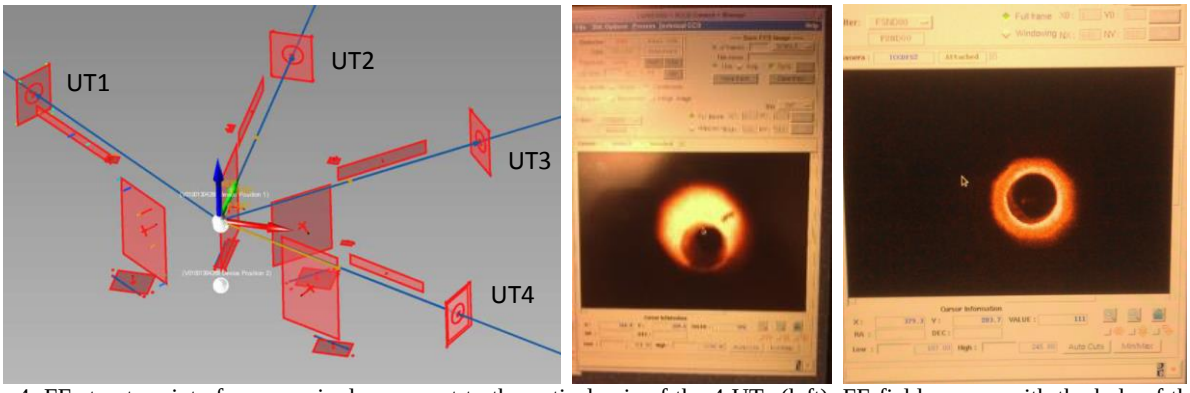

Figure 4: FE structure interfaces acquired as respect to the optical axis of the 4 UTs (left); FE field camera with the hole of the star fiber misaligned as respect to the calibration light (center); FE field camera with the hole of the star fiber aligned and in focus as respect to the calibration light (right).

Concerning the last point, the single Fiber Link heads were aligned with shims by centering the star holes with the calibration spot, with the Field camera as feedback (Figure 4). A minimization of the errors was performed for the HR and UHR heads, being the same for all UTs, while a larger freedom was possible for the MR heads, which are aligned to the respective telescope only.
In order to maximize the coupling efficiency into the spectrograph fibers, their pupils were aligned to the telescope pupil at the ADC level by setting an offset in the rest position of the pupil mirror of each FE unit. These corrections were necessary, since uncertainties were present on the relative angle between the fibers axis and the mechanical reference on the Fiber Link heads. We considered the ADC frame, aligned to the nominal position to better than 1 mm during the installation of the Coudé trains, as the centre of the telescope pupil, and we visualized the fiber pupil by shining the light from the other head of the fiber (at the scrambler link). A maximum correction of 12% (8% RMS) of the piezo range was applied to properly centre the fiber pupils to the telescope pupils in the different observing modes.

3. ANAMORPHIC PUPIL SLICER UNIT

The Anamorphic Pupil Slicer Unit (APSU)[8] is the spectrograph preslit unit, used to increase the spectrograph resolving power, effectively decreasing the slit width. Two cylindrical objectives with different focal lengths introduce the anamorphism; the slicer, composed by two (almost) achromatic couple of prisms likely configured as a Risley prisms pair, cut the pupil in two, and introduce horizontal and vertical tilt to shift the image of the two pupils on the APSU focal plane; the Multi-Mini Prism (MMP), composed by twelve round-base prisms (1 or 2 mm in diameter by 2 mm in height), are placed in the focal plane to fold the light and overlap the pupils onto the echelle grating.

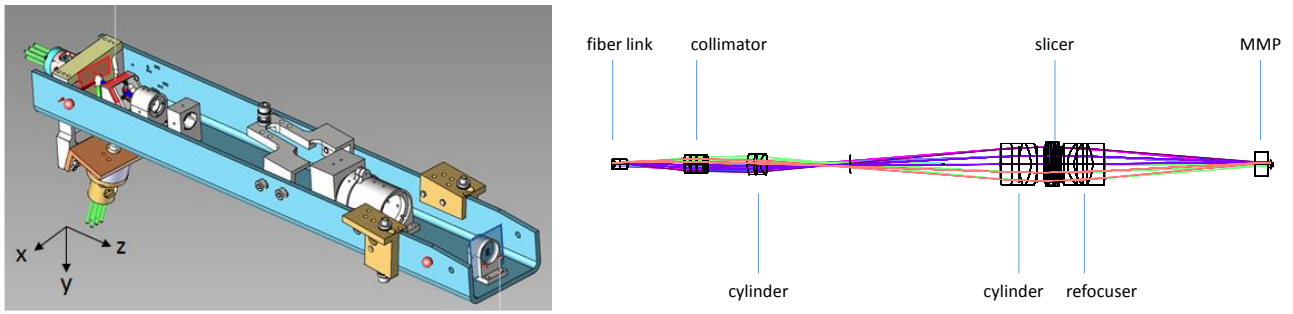

Figure 5: APSU mechanical design; reference spheres are also shown in red (left). Optical design (right).

3.1 Alignment strategy

The alignment strategy consisted in the fabrication of the mountings with tight tolerances on the optics barrels. Any mounting was characterized with the CMM, and its optical axis was referenced with six points on the mounting. The same six points were used to align via CMM the single mountings on the APSU bench, by shimming, using the external spheres on the APSU bench as global reference points (Figure 5). Accuracies below 10 um in the positioning of the six reference points were obtained. This procedure was followed for all the main components, but in few cases, where the accessibility was low or the optics degree of freedom was not measurable on the mountings, we were forced to support this technique with optical methods.

3.2 Slicer alignment

The centration of the slicer and its clock around the optical axis are critical, influencing the relative alignment and relative power between the images of the two slices on the detector. A shift between the two slices in the main dispersion direction translates into a decrease in spectral resolution when the two slices are extracted as a single line (with a binning in the cross-dispersion direction); a difference in the relative power results in a non optimal extraction of the signal from the data reduction pipeline, with consequences on the SNR between the two lines or possible saturation in the most intense line. The close packing of the slicer between the second cylinder and the refocuser did not allowed the use of mechanical only alignment techniques. We therefore estimated the position and balancing of the two half pupils by measuring their size and position with millimeter paper, and analyzing the pictures with imaging software (as ImageJ). Even if the method is incredibly simple, sub-millimeter alignment precision is reachable, and the two slices were perfectly equilibrated within the detector measurement noise (Figure 6). Concerning their relative position in the main

dispersion direction on the spectrograph detector, a relative shift occurs when the system is evacuated. Accordingly, few clock adjustments around the optical axis of the slicer in the order of 0.1° were iteratively performed until a shift in the order of the pixel was observed.

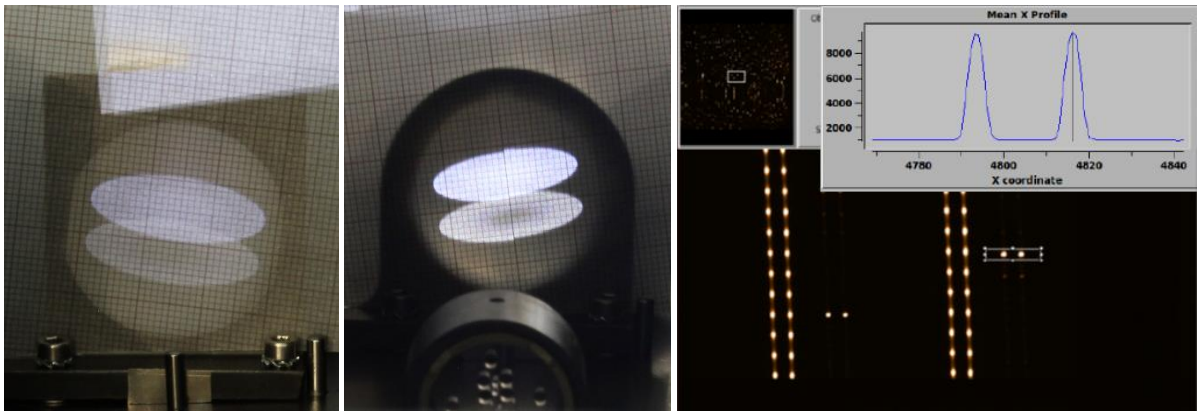

Figure 6: pupils of the star and sky fibers in the UHR mode before (left) and after (center) the slicer. Part of the CCD image (right) showing two diffraction orders (Fabry-Perot on sky fiber and Th-Ar on star fiber); the two traces per order are the images of the two slices. In the inset the profile of two slices of the star fiber.

3.3 MMP and Fiber Link alignment

The MMP was integrated at INAF - Brera observatory in Merate by gluing the single prisms onto the silica substrate. Details of the methods and procedures for the production and verification of the MMPs (Figure 7) can be found in a previous paper[12]. The MMP#3 was aligned into the APSU in the nominal position by combining optical and mechanical characterizations; then, in the same way, the Fiber Link was optically aligned to the MMP. This strategy was necessary since the mechanical referencing of the Fiber Link for all the degrees of freedom was possible. The following procedure was followed:

- miniprisms relative positions on the silica substrate were determined with a custom-developed software from images taken with a CCD camera equipped with a 230 mm focal length objective, as reported in Figure 7; an RMS error of 58 um was obtained, where the two main players were prisms #8 and #12;
- the device was inserted in the mounting, roughly aligned at 8 deg clock, glued and installed in the APSU;
- the camera was placed in front of the APSU, to image the MMP in the APSU;
- with images (Figure 8) the two reference holes in the mounting were referenced to the miniprisms;
- the MMP was aligned in the APSU with the articulated arm by measuring the position of the two holes in the mounting and the substrate surface. We obtained the following errors (reference system in Figure 5):

x	-0.012	mm
y	-0.059	mm
z	-0.019	mm
tx	-3.15	arcmin
ty	1.50	arcmin
tz	-4.60	arcmin

- Fiber Link 2 was mounted on the APSU, and aligned in z (50 um), tx and ty (0.1 and 0.7') with the articulated arm. The alignment was completed by visualizing the virtual slit on the MMP plane, as shown in Figure 8, injecting the light into the optical fibers.

With this combined procedure we ensured a positioning accuracy of the Fiber Link and MMP of less than 100 um for the translations and 5 arcmin for the rotations. To verify the mutual centering between the fiber entrance and the miniprisms we measured the transmission efficiency of the MMPs of the different fibers by injecting white light (halogen) in the single fibers and measuring the light power with a power meter (Ophir PD300UV) placed before and after the MMP plate. The obtained results confirmed a good alignment (Figure 8), where the 2% loss is probably due to the coating on the substrate and on the miniprisms surface. Concerning the Multi MR mode, the larger loss is present by design, due to the cut of the image corners by the miniprisms.

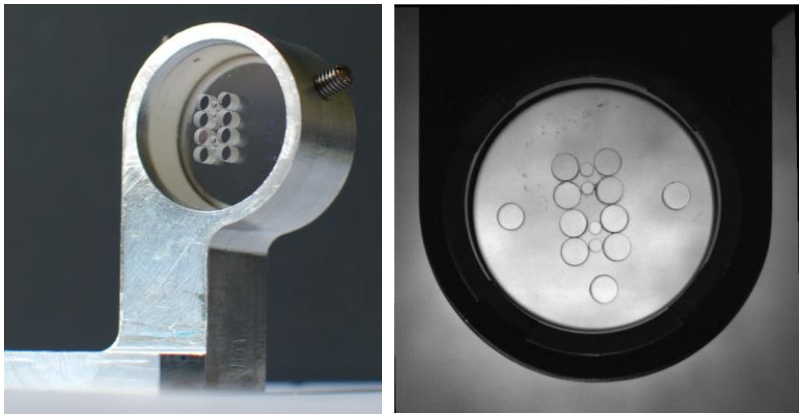

Figure 7: first MMP prototype (left). MMP#3 (center), now installed in the spectrograph, in the final mounting; the three external prisms are used as reference. A similar image was used to determine the prism relative position. Prisms positions (right) obtained by best fit of the measured positions (blue) and the theoretical ones (red).

Mode	# MMP	Fiber	efficiency
UHR	1-7	A	98.0%
UHR	2-8	B	98.0%
HR	5-11	A	98.5%
HR	6-12	B	98.0%
MR	3-9	A	97.0%
MR	4-10	B	96.0%

Figure 8: MMP#3 during integration in the APSU. Enhanced brightness image to show the mechanical references in the mounting (left); virtual slits on the MMP plane: four images for each observation mode, made by star and sky fibers, sliced in two (center); transmission efficiency of the single fibers (right).

3.4 APSU alignment on the optical bench

Concerning the alignment of the APSU on the optical bench, we verified no possibility to align it on the three reference spheres with the laser tracker. We therefore considered a combined method, employing also the articulated arm. The latter was mounted on the bench, along with three nests in the measurement range of both instruments. The retroreflectors were measured with the laser tracker and the articulated arm, so that the articulated arm was referenced to the optical bench. The APSU was then aligned with the articulated arm only with the usual shimming method. Given the two step process, we expected positioning errors larger than 100 um for the single reference spheres, corresponding to about 2' in the tilt along the horizontal and vertical directions.

The verification was performed visualizing the beam pupil at both the MC, with a paper mask obtained from the optical cad (see Figure 9), and the ECH. We observed an error of 11' in the tilt along the vertical axis. The tilt along the horizontal axis was within the verification accuracy. After the application of the correction (0.6 mm shim on 200 mm lever) the pupils were correctly centered on both the MC and ECH (Figure 10). The APSU was placed in the nominal position for what concerns the translations, and the residual defocus in both channels was corrected with the two transfer collimators (corresponding to -0.8 mm in the APSU axial position).

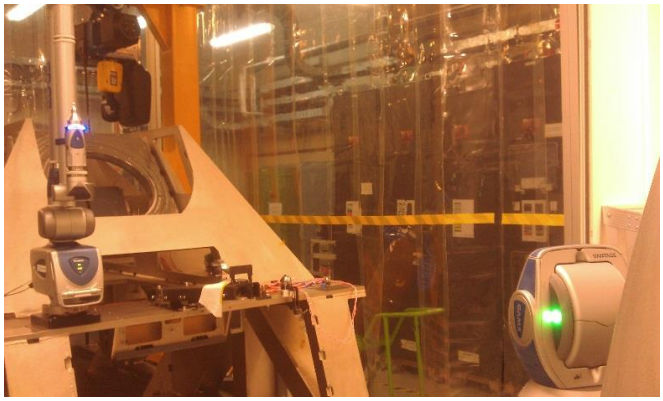

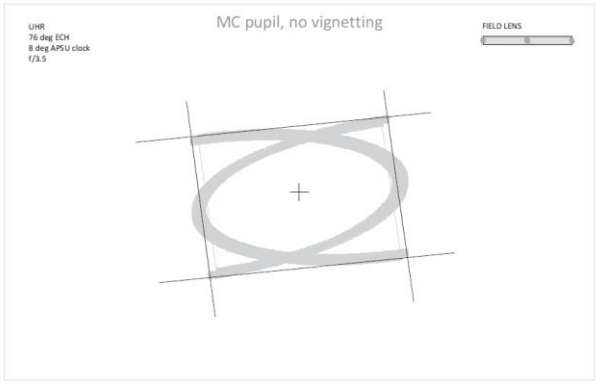

Figure 9: the laser tracker and the articulated arm mounted on the optical bench in the CCL at Paranal (left). The MC mask (right).

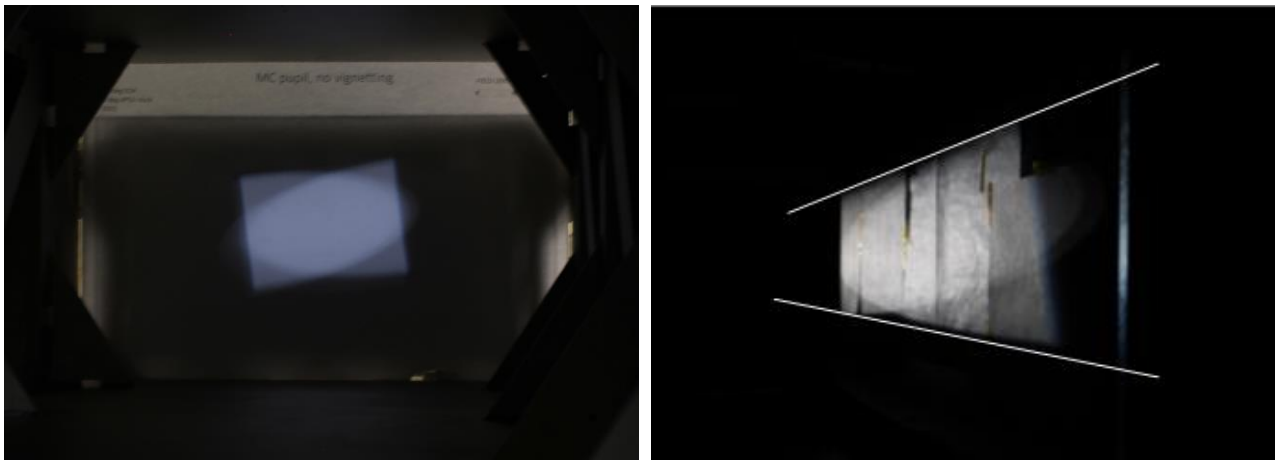

Figure 10: pupil on the MC (left) and on the ECH cover (right); the white lines mark the ECH edges.

4. SPECTROGRAPH

To guarantee long term instrument stability, the optics mountings have been designed without actively controlled alignment. This means that alignment is achieved by manufacturing accuracy and monitoring throughout the instrument development, both for the optical and the mechanical design[9]. The optics have been referenced to the mounting interfaces by using the CMM, to obtain a micrometer level measurement precision, while the corresponding mounting interfaces were referenced to the optical bench using the LT (Vantage). After integration of the optics on the optical bench, the position of accessible optical components was cross-checked by measuring the non-optical surfaces with the LT, obtaining differences from the nominal positions well within 0.1 mm. For the most internal optics, like the field lens/mirror and the dichroic the cross check was not possible.

In general, the optics misalignments sum up along the optical train, and any mechanical misalignment is emphasized when the optics is reflective. In our case, approximately ten elements are present in each channel, and lots of them are reflective, working either in single or double pass; accordingly, any misalignment is doubled one or two times by each component.

We observed on the two CCD cameras two main effects:

- a shift in the echellogram position, due to a tilt of the optical components positioned near a pupil; this effect was corrected acting on the tilt of the corresponding TC;
- an image defocus, differential between the two channels, and a non-uniform optical quality; this effect was corrected with a translation of the component placed near the intermediate focus of each channel, either the dichroic mirror for the blue channel and the field mirror for the red channel.

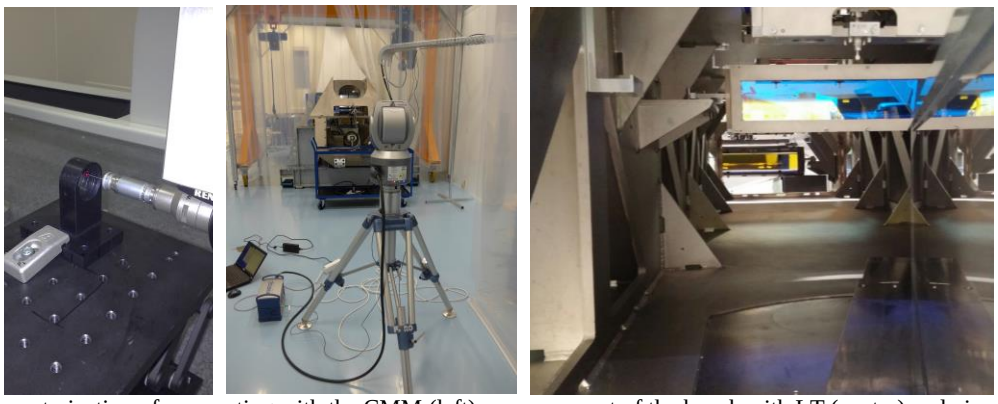

Figure 11: characterization of a mounting with the CMM (left), measurement of the bench with LT (center) and view of the bench with the echelle grating, main collimator and dichroic (right).

4.1 Echellogram position on the CCD

The residual tilt in the components placed near a pupil and in the camera flange for both channels induced a decentering in the echellogram position on the CCD, where the detector sensitivity is maximized and the contribution of space-variant noises (like the Dark Current for some family of CCD) is reduced. We show here the example of the blue channel, where the decentering can be easily identified on the detector since the echellogram is cut by the field lens and only the free spectral range is transmitted (Figure 12). We observed a horizontal shift of about 230 pixels in the echellogram format, corresponding to a tilt in the camera optical axis of 20 arcmin. Since we could not act on the camera to correct this tilt, we applied the corresponding tilt to the TC (calculated from the sensitivity analysis[13] and performed with shimming on the TC mountings), after the verification with the ray-trace software that no degradation would have occurred in the image quality. Figure 12 shows the simulated spectral format and the raw frame of the blue CCD after the realignment process.

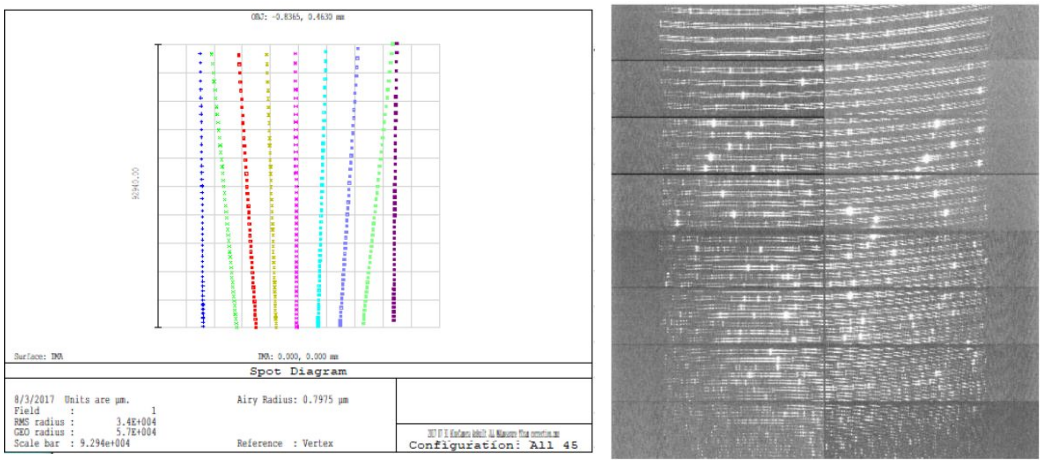

Figure 12: simulated spectral format for the nominal condition (left) and raw blue frame in HR mode with Th-Ar lamps on both fibers (right).

4.2 Image defocus and optical quality uniformity

Image defocus in the spectrograph was observed for both channels, complicated by the focal shift between the in-air and vacuum conditions, where the instrument is aligned and operated, respectively. Moreover, we observed a non-uniform image quality throughout the CCD, with a degradation of the enslitted energy in the main dispersion direction only in the reddest wavelengths of each order.

In principle, a focal degradation could be corrected by misplacing any element in the optical train along the optical axis, included the source itself (APSU), but only few elements are responsible for the image non-uniformity in the main dispersion direction only. In particular we identified with ray-tracing analysis the dichroic mirror (DM) as the possible

responsible for this effect in the blue channel, and the field mirror (FM) in the red channel. Accordingly, we applied the shims on the DM and FM of 2.2 mm and 1.6 mm, respectively, obtaining a more uniform image quality on all chip.
The good image quality obtained is proven by the resolution maps measured in Paranal during the commissioning, in March 2018. Although small wavelength zones have been clipped by the DRS, in the blue channel the upper envelope reaches a resolving power of R = 215'000, while in the red channel R = 235'000 is commonly obtained and even exceed in the very red end of the spectrum (Figure 13). For completeness we also show the resolving power obtained for the HR mode, where the resolving power defined by the upper envelope data points lies between R = 145'000 and R = 155'000, well above the specs. We suspect that the higher resolution as respect to the design, for both UHR and HR, is due to the low flux on the Th-Ar exposure which returns a slightly smaller FWHM than designed.

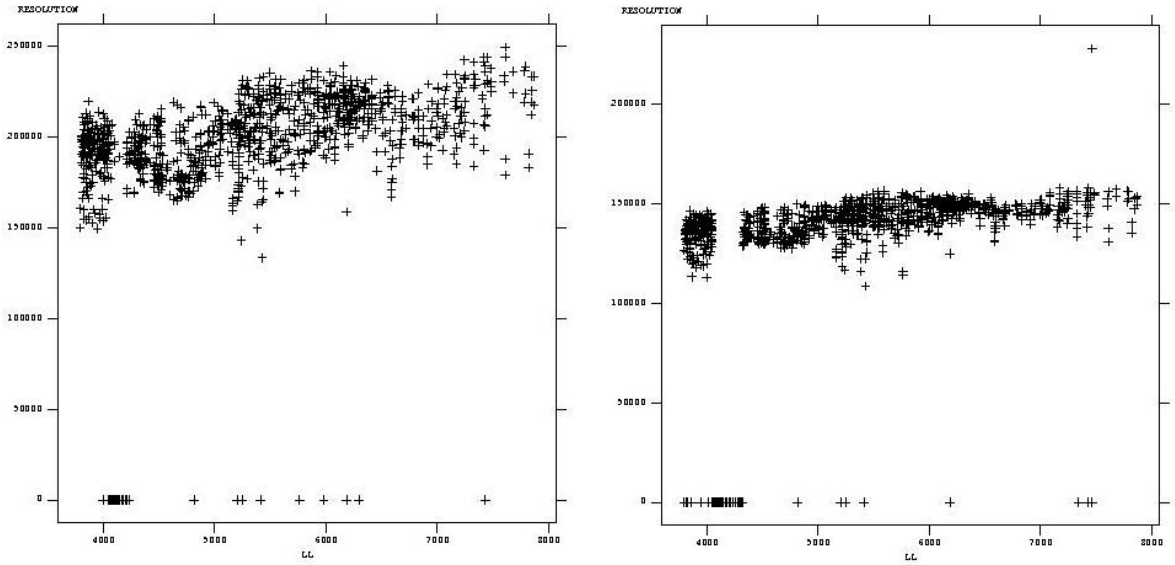

Figure 13: resolution plot as function of the wavelength for the UHR (left) and HR (right) modes.

5. CONCLUSIONS

We described the methods followed and the optical verifications performed during the integration of ESPRESSO, the high resolution spectrograph now under the commissioning phase at Paranal Observatory on ESO's Very Large Telescopes. The 'blind' alignment method is a powerful technique to effectively integrate large optical system, to bring the system in the almost nominal conditions. We highlighted the limitations of this method in specific cases, where optical verifications can easily be integrated (for non accessible or small components). Final instrument performances have been presented, demonstrating the effectiveness of this approach.

REFERENCES

[1] Pepe, F. A., Cristiani, S., Rebolo Lopez, R., Santos, N. C., Amorim, A., Avila, G., Benz, W., Bonifacio, P., Cabral, A., et al., "ESPRESSO: the Echelle spectrograph for rocky exoplanets and stable spectroscopic observations," Ground-based Airborne Instrum. Astron. III. Ed. by McLean **7735**, 14 (2010).

[2] Mégevand, D., Zerbi, F. M., Cabral, A., Di Marcantonio, P., Amate, M., Pepe, F., Cristiani, S., Rebolo, R., Santos, N. C., et al., "ESPRESSO, the ultimate rocky exoplanets hunter for the VLT," Proc. SPIE **8446**, 84461R 1-15 (2012).

[3] Mégevand, D., Zerbi, F. M., Di Marcantonio, P., Cabral, A., Riva, M., Abreu, M., Pepe, F., Cristiani, S., Rebolo Lopez, R., et al., "ESPRESSO: the radial velocity machine for the VLT," Proc. SPIE **9147**, 91471H 1-18 (2014).

[4] Cabral, A., Abreu, M., Coelho, J., Gomes, R., Monteiro, M., Oliveira, A., Santos, P., Ávila, G., Delabre, B.-A., et al., "ESPRESSO Coudé-Train: Complexities of a simultaneous optical feeding from the four VLT unit telescopes," Proc. SPIE **9147**, 91478Q 1-11 (2014).

[5] Riva, M., Aliverti, M., Moschetti, M., Landoni, M., Dell'Agostino, S., Pepe, F., Mégevand, D., Zerbi, F. M., Cristiani, S., et al., "ESPRESSO front end: modular opto-mechanical integration for astronomical instrumentation," Proc. SPIE **9147**, 91477G 1-9 (2014).
[6] Riva, M., Landoni, M., Zerbi, F. M., Mégevand, D., Cabral, A., Cristiani, S.., Delabre, B., "ESPRESSO front end opto-mechanical configuration," Proc. SPIE **8446**, 84469E 1-7 (2012).
[7] Spanò, P., Delabre, B., Dekker, H., Pepe, F., Zerbi, F. M., Di Marcantonio, P., Cristiani, S.., Mégevand, D., "Very high-resolution spectroscopy: the ESPRESSO optical design," Proc. SPIE **8446** (2012).
[8] Conconi, P., Riva, M., Pepe, F., Zerbi, F. M., Cabral, A., Cristiani, S., Megevand, D., Landoni, M.., Spanó, P., "ESPRESSO APSU: simplify the life of pupil slicing," Proc. SPIE **8842**, 88420P 1-9 (2013).
[9] Tschudi, S. S., Fragoso, A., Amate, M., Mégevand, D., Tschudi, S. S., Fragoso, A., Amate, M., Rebolo, R.., Mégevand, D., "Design of the opto-mechanical mounts of the ESPRESSO spectograph," Proc. SPIE **9151** (2014).
[10] Aliverti, M., Pariani, G., Moschetti, M.., Riva, M., "Integration and alignment through mechanical measurements: the example of the ESPRESSO front-end units," 99087C (2016).
[11] Pariani, G., Aliverti, M., Moschetti, M., Landoni, M., Riva, M., Zerbi, F. M., Mégevand, D., Cristiani, S.., Pepe, F., "Integration, alignment, and verification of the ESPRESSO Front-End," 99087B (2016).
[12] Oggioni, L., Pariani, G., Moschetti, M., Riva, M., Genoni, M., Aliverti, M.., Landoni, M., "MMP, the Multi Mini Prism device for ESPRESSO APSU: prototyping and integration," 990872 (2016).
[13] Genoni, M., Riva, M., Pariani, G., Aliverti, M.., Moschetti, M., "Spectrograph sensitivity analysis: An efficient tool for different design phases," Proc. SPIE - Int. Soc. Opt. Eng. **9908** (2016).